

## Measurement of Dose Distribution in Small Beams of Philips 6 and 8 MVX Linear Accelerator

Tae-suk Suh, Ph.D., Sei Chul Yoon, M.D.  
Kyung Sub Shinn, M.D. and Yong Whee Bank, M.D.

*Department of Radiology, Catholic University Medical College, Seoul, Korea*

The work suggested in this paper addresses a method for collecting beam data for small circular fields. Beam data were obtained from Philips 6 and 8 MV LINAC at Dept. Radiation Therapy at Gainesville Incorporated and Shands Teaching Hospital. Specific quantities measured include tissue maximum ratio (TMR), off-axis ratio (OAR) and relative output factor (ROF).

In small field irradiation, special collimators were used to produce circular fields of 1 cm to 3 cm diameter in 2 mm steps, measured at SAD (source axis distance) of 100 cm. Diode detector was chosen for primary beam measurement and compared with measurements made with photographic film and TLD dosimeters.

The measured TMRs and OARs were formulated from limited measurements to generate basic beam data for reference set-up. The empirical formulae were later, extended and generalized for any possible set-up using the trends of fitting parameters. The measured TMRs and OARs were well represented by the fitting formula developed.

---

**Key Words:** Small field irradiation, LINAC, beam measurement

### INTRODUCTION

Small field beams measurement is prerequisite for the treatment of small intracranial targets. The measurement data for tissue-maximum-ratio (TMR) and off-axis ratio (OAR) are the main function data for the isocentric treatment, which is used for LINAC-based stereotactic radiosurgery. The concept and mechanical design of stereotactic radiosurgery using LINAC were described in many literatures<sup>1-6</sup>.

The effort to measure small beams has been reported in several papers<sup>7,8</sup>. A detailed analysis for dose measurements and accuracy of the measured dose in small fields was fully discussed in Rice et. al<sup>9</sup>. Since lateral electronic equilibrium is not complete for small beam measurement, small detector should be used to achieve high spatial resolution. Several detectors should be evaluated to test the relative accuracy and convenience of measurements.

Small beam measurement presents another problem. Special consideration and good accuracy are necessary in finding the central axis point and moving the detector in small steps for small

field. It is very tedious and time-consuming job to acquire the enormous beam data through measurement for all the possible treatment set-ups.

The purpose of this work is to develop basic beam data collection method for small field to estimate TMR and OAR for any possible treatment set-up from the limited measurements.

### MATERIALS AND METHODS

#### 1. Special Collimator

The measurement was performed for small circular field using the special collimator made by cerrobend. For this purpose cylindrical collimators were used with small holes to produce circular fields of 1 cm to 3 cm diameter in 2 mm steps, measured at SAD of 100 cm. The opening was tapered to match beam divergence and thereby further minimizing the penumbra. The diameters of upper and bottom holes of that cylindrical collimator can be obtained from geometrical calculation.

#### 2. Dose Model

Most of computing technique used for the dosage calculation and beam data are based on the beam model. We discuss the dose model and beam measurement for a fixed single beam. This is basic background for developing an efficient 3-D dose

---

This paper was supported by 1991 CUMC Clinical Medical Research Fund.

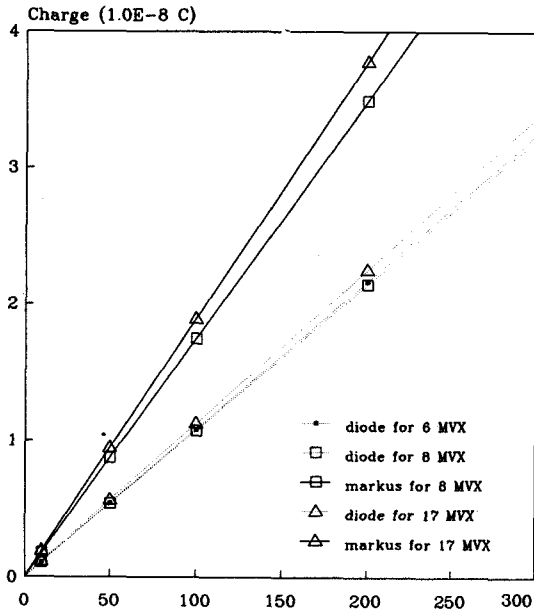


Fig. 1. Detector response versus dose for a number of energies.

algorithm for multiple moving beams. The 3-D dose algorithm for multiple moving beams will be discussed elsewhere in the future.

A simple empirical isocentric model<sup>(8,9)</sup> will be modified to describe the dose for circular field treatment. An isocentric model for single circular treatment is given by

$$D_m(C, STD, d, r) = D_{ref} \times ROF(C) \times TMR(w, d) \times (SAD/STD)^2 \times OAR(C, STD, d, r) \quad (1)$$

where

- m = point of interest in a medium
- C = collimator size defined at SAD
- STD = source to target distance
- w = field size at point of interest m expressed by  $w = C (STD/SAD)$
- d = depth of point of interest m
- r = off-axis distance
- SAD = source to axis distance = 100 cm
- $D_m$  = the dose at point of interest m
- $D_{ref}$  = the dose for the reference set-up
- ROF = relative output factor defined by  $D(C, STD=100, d_m, r=0) / D(C_{ref}, SSD=100, d_m, 0)$
- TMR = tissue maximum ratio defined by  $D(w, d) / D(w, d_m)$
- OAR = off-axis ratio defined by  $D(C, STD, d, r) / D(C, STD, d, r=0)$

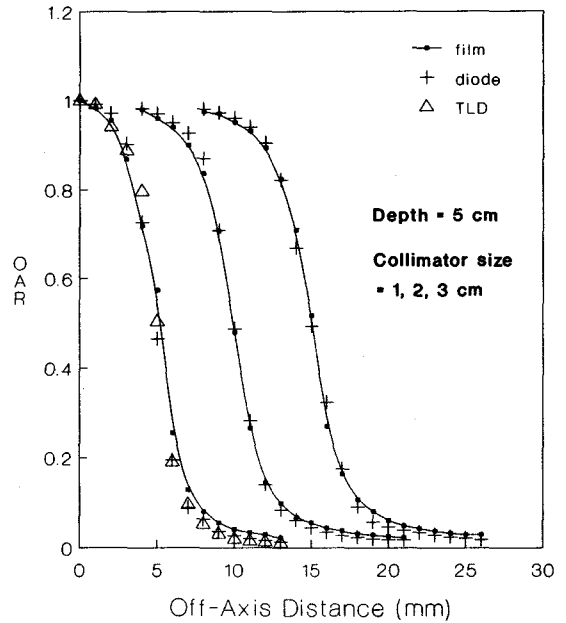


Fig. 2. Off-axis ratio for field sizes of 1, 2, and 3 cm (SAD=100 cm) scanned at depth of 5 cm in solid water using film, diode and TLD.

The measurement data for tissue maximum ratio (TMR) and off-axis ratio (OAR) are the main function data for the dose model developed. These measurements are identified as basic beam data. Our task for small beam measurement with above dose model included two main parts. The first part was to determine the detector system for our small beam measurement. The second part was to formulate basic beam data from our limited measurements.

### 3. Detector System

While we tested many detectors (e.g., iso-octane liquid ion chamber, Markus ion chamber, TLD, film and diode), the diode detector was chosen as our primary beam measurement device due to the good characteristics and the small size of the sensitive volume (2 mm diameter). Fig. 1 shows good detector response while representing the linear relationship between diode reading and dose for various x-ray beam energies. Fig. 2 shows the good agreement between the diode and other detectors (film and TLD) for the OAR measurement.

### 4. Formulation of Basic Beam Data

The effort to formulate the percentage depth dose, output factor and beam profile was made for

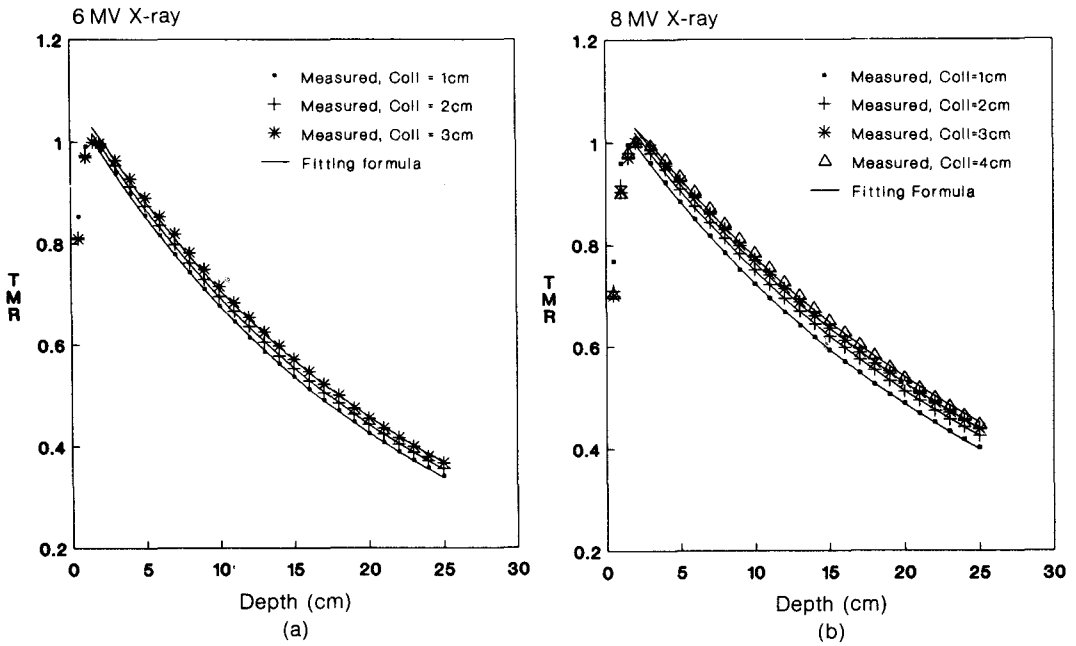


Fig. 3. Tissue-maximum-ratio for 6 MeV X-ray (a) and 8 MeV X-ray (b). The points denote the measured beam data and the curves denote the analytic function.

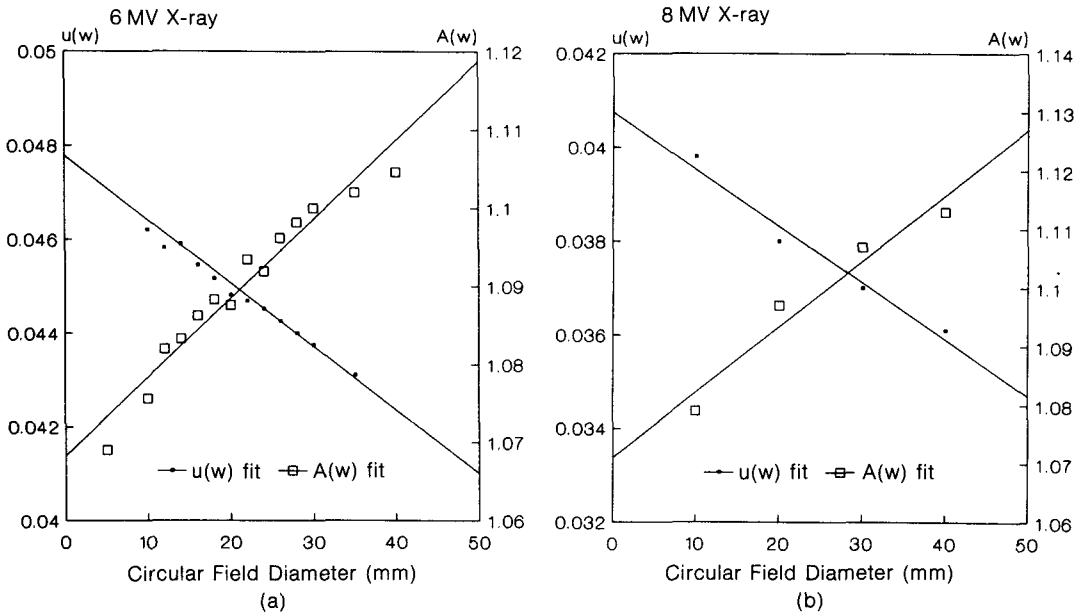


Fig. 4. Fitting parameters of TMR function, A and  $\mu$  vs. collimator settings for 6 MeV X-ray (a) and 8 MeV X-ray (b). Collimator setting define the field size at isocenter (SAD=100 cm).

the normal rectangular collimator size in the previous reports<sup>7,10,11</sup>. The formulation of the TMR for

the small circular collimator was described in Rice et al.<sup>8</sup> In order to formulate both the TMR and OAR,

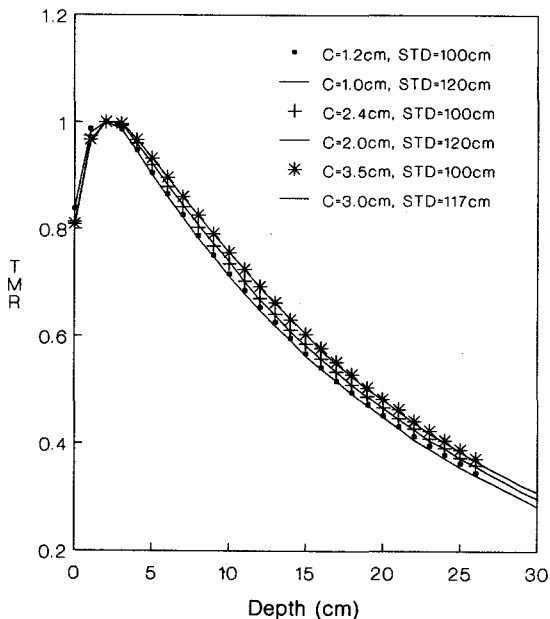


Fig. 5. Tissue maximum ratio for different source-to-target distance (STD). The points represent the TMR for 100 cm of STD and the curves represent the TMR for 120 cm of STD.

for any real treatment setup from a limited number of dose measurements, were obtained from the reference set-up. Then the possible empirical formula were used to fit the data. Those formulae were later extended and generalized for any real treatment setup by finding the relationship between fitting parameters and beam parameters. Empirical formulae for 6 MVX at Radiation Therapy at Gainesville institute and 8 MVX at Shands Teaching Hospital were derived to represent TMR and OAR for any real treatment setup from a limited number of dose measurements.

**RESULTS AND DISCUSSION**

**1. Tissue Maximum Ratio**

The TMR was measured from the fixed source to chamber (or source to target) distance, 100 cm to the diode and build-up of solid water. Fig. 3 shows trends of TMR data measured (data points) for two different X-ray beams. TMR data were fit to a function of the form beyond the build-up region ( $d_{max} = 1.5$  cm for 6 MVX or 2 cm for 8 MVX):

$$TMR(STD, C, d) = A(C) \times \exp(-\mu(C) \times d) \dots\dots\dots(2)$$

where  $\mu(C)$  is the effective linear attenuation coefficient in water for collimator field size C, and A (C) allows one to account for the shift in  $d_{max}$  with field size. The curves in figure 3 represent the fit of TMR data for 1, 2, 3 and 4 cm collimator sizes. Fig. 4 shows a plot of A and  $\mu$  values as a function of collimator field size. The values for A and  $\mu$  are scattered in a linear fashion. Fig. 5 shows plots of TMR vs. depth for different source-to-target distances. These show a good agreement (to within 1%) between the TMR obtained from the different source-to-trarget (STD) distances. Since TMR is independent of source to target distance and dependent on field size  $w_d$  at depth d, the formula for TMR can be expressed by

$$TMR(w, d) = A(w) \times \exp(-\mu(w) \times d) \dots\dots\dots(3)$$

where

$$A(w) = A_1 + A_2 w \dots\dots\dots(4)$$

$$\mu(w) = \mu_1 + \mu_2 w \dots\dots\dots(5)$$

$$w = C \times SAD, SAD=100 \text{ cm} \dots\dots\dots(6)$$

and  $A_1, A_2, \mu_1$  and  $\mu_2$  are coefficients of linear regression, and are shown in Table 1.

Fig. 6 shows the TMR trends at or near  $d_{max}$  for 6 MVX for both STD=100 and STD=90 using film measurement. The values of TMR for the larger field size are slightly smaller than those for the smaller field size in the region below  $d_{max}$ , and vice versa beyond  $d_{max}$ . It is possible to derive an empirical formula for TMR within the build-up region. Since the difference of TMR among the different collimator sizes is small, it is desirable to obtain an approximate formula for all the collimators in the build-up region such as cubic polinomial fit.

It is hown that the measurement of TMR for 8 MVX gives trends similar to those of 6 MVX.

**2. Off-Axis Ratio**

OARs were measured with the diode at  $d_{max}$  and at 10 cm depth FOR 6 MVX and 8 MVX beams while using varying combinations of collimators and source-to-target distances. Fig. 7 show the result of OAR measurements for diffent collimator field sizes at  $d_{max}$  and 10 cm depth with fixed STD of 100 cm.

Since the difference between OARs at depth at any off-axis distance is small, any profile dependence on depth can be ignored for normal clinical applications. The curves in Fig. 7 represent multi-depth fits for each collimator using the modified Cunningham model:

$$OAR(STD, C, r) = 1 - 0.5 \times \exp[-\alpha_1 \times (w_d/2 - r)/p - \beta \times (w_d/2 - r)^2/p^2] \text{ for } r \leq w_d/2 \dots\dots\dots(7a)$$

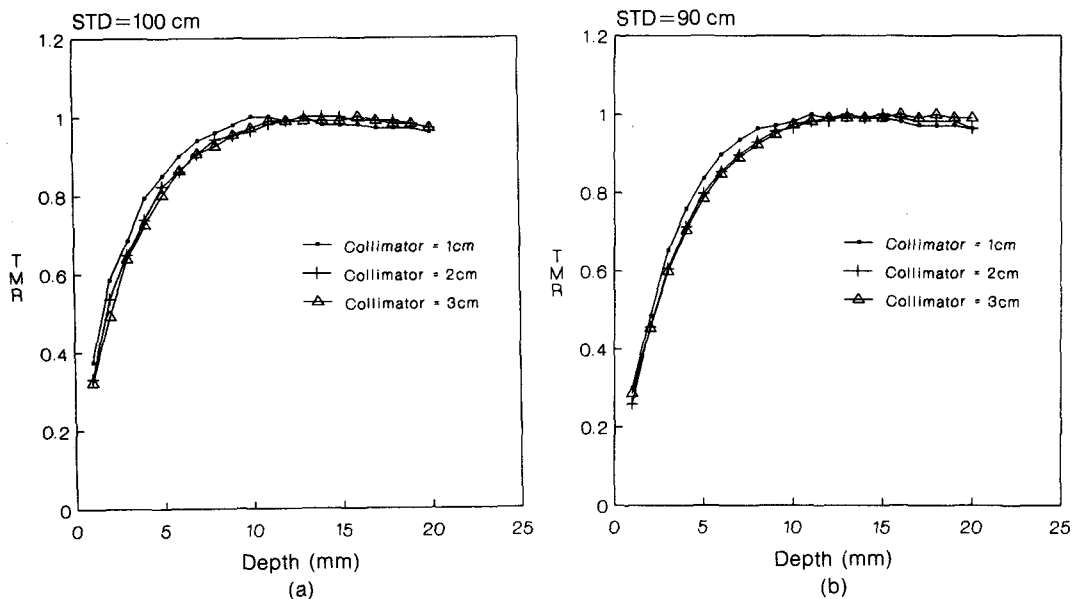
$$= t + (0.5 - t) \times \exp[-\alpha_2 \times (r - w_d/2)/p]$$

**Table 1.** Table of Fitting Parameters for TMR

| Collimator size (cm) | 6 MeV |        | 8 MeV |        |
|----------------------|-------|--------|-------|--------|
|                      | A     | $\mu$  | A     | $\mu$  |
| 1.0                  | 1.076 | 0.0462 | 1.079 | 0.0398 |
| 1.2                  | 1.080 | 0.0458 |       |        |
| 1.4                  | 1.083 | 0.0459 |       |        |
| 1.6                  | 1.086 | 0.0455 |       |        |
| 1.8                  | 1.088 | 0.0452 |       |        |
| 2.0                  | 1.088 | 0.0448 | 1.097 | 0.0380 |
| 2.2                  | 1.093 | 0.0447 |       |        |
| 2.4                  | 1.092 | 0.0445 |       |        |
| 2.6                  | 1.096 | 0.0442 |       |        |
| 2.8                  | 1.098 | 0.0440 |       |        |
| 3.0                  | 1.100 | 0.0437 | 1.107 | 0.0370 |
| 3.5                  | 1.102 | 0.0431 |       |        |
| 4.0                  | 1.105 | 0.0427 | 1.113 | 0.0361 |

| Energy | $A_1$ | $A_2$  | $\mu_1$ | $\mu_2$  |
|--------|-------|--------|---------|----------|
| 6 MeV  | 1.068 | 0.0101 | 0.0478  | -0.00135 |
| 8 MeV  | 1.071 | 0.0112 | 0.0407  | -0.00121 |



**Fig. 6.** Tissue maximum ratio in build-up region for two different of STD, 100 cm (a) and 90 cm (b) using film.

$$\text{for } r > w_d/2 \dots (7b)$$

where  $w_d$  is given by Eq. 6, and  $r$  represents off-axis distance. penumbra,  $p$ , is expressed by

$$p = SS \times (STD - SCD) / SCD \dots (8)$$

Figure 8 shows OAR beam data at  $d_{max}$  and 10 cm depth with the respective formula generated

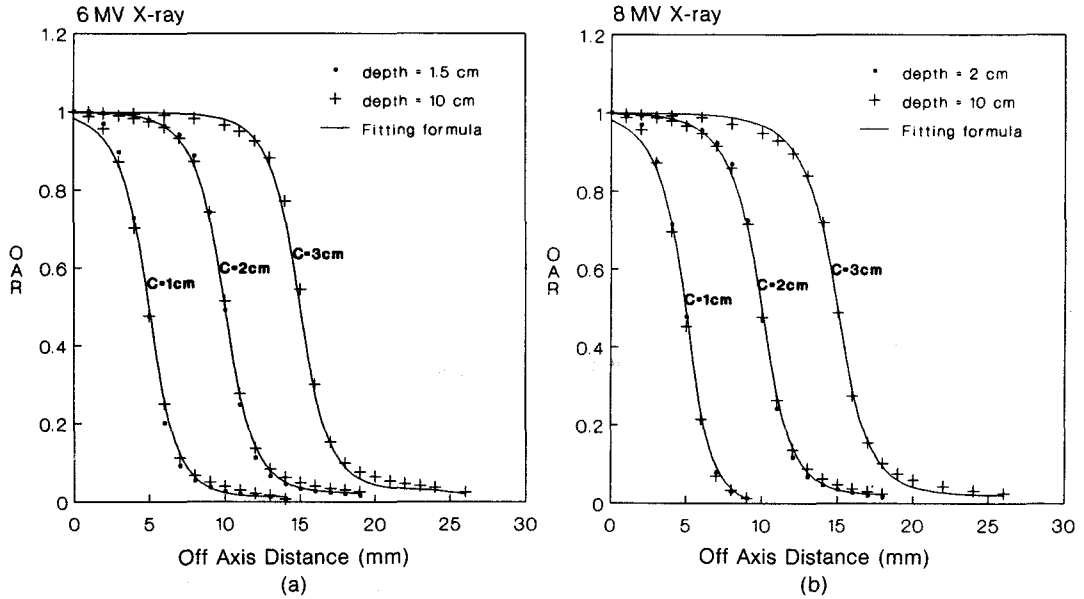


Fig. 7. Off-axis-ratio for 6 MeV X-ray (a) and 8 MeV X-ray (b). The points represent the measured beam data for collimator sizes of 1, 2 and 3 cm at depths of  $d_{max}$  and 10 cm with fixed STD of 100 cm. The curves denote fitting formula.

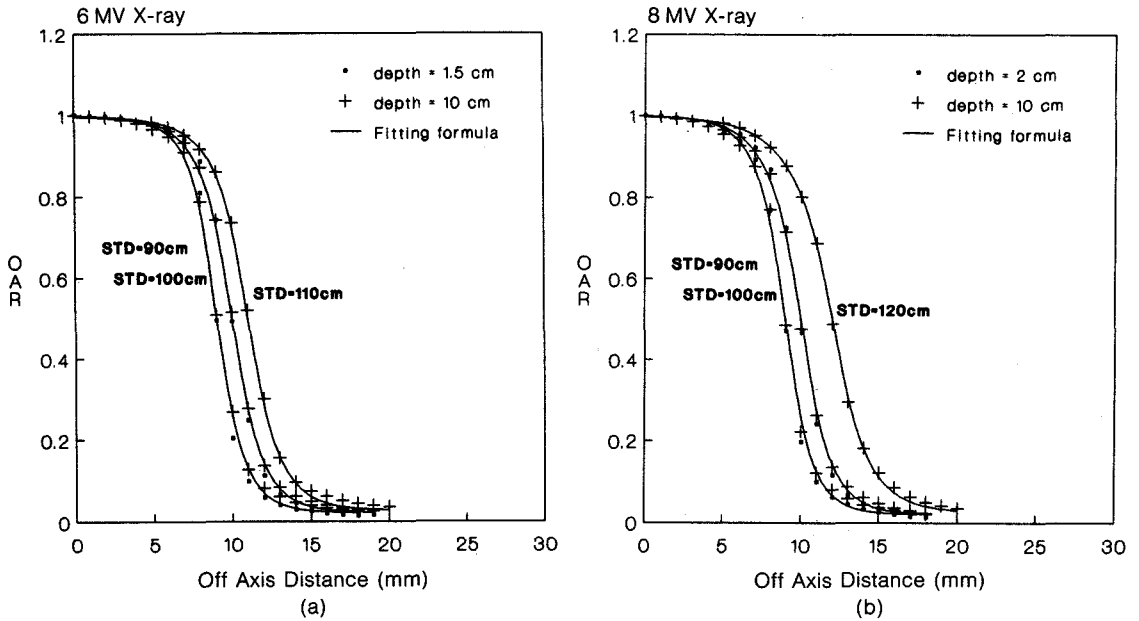


Fig. 8. Off-axis-ratio for 6 MeV X-ray (a) and 8 MeV X-ray (b). The points represent the measured data at  $d_{max}$  and 10 cm depth for three different STDs with a collimator size of 2 cm. The curves denote fitting formula.

curves for three different STDs with a collimator size of 2 cm. The same accuracy of fit was obtained

from fitting formula with other collimators. Since transmission dose not change much, the constant

**Table 2.** Table of Fitting Parameters for OAR

| Collimator size (cm) |         | Source to Target Distance (cm) |        | 6 MVe      |            |         |
|----------------------|---------|--------------------------------|--------|------------|------------|---------|
|                      |         |                                |        | $\alpha_1$ | $\alpha_2$ | $\beta$ |
| 1.2                  |         | 83                             |        | 0.252      | 0.372      | 0       |
|                      |         | 100                            |        | 0.524      | 0.613      | 0       |
|                      |         | 114                            |        | 0.246      | 0.953      | 0       |
| 2.0                  |         | 90                             |        | 0.498      | 0.457      | 0       |
|                      |         | 100                            |        | 0.581      | 0.629      | 0       |
|                      |         | 110                            |        | 0.740      | 0.773      | 0       |
| 2.8                  |         | 92                             |        | 0.523      | 0.463      | 0       |
|                      |         | 100                            |        | 0.633      | 0.583      | 0       |
|                      |         | 107                            |        | 0.696      | 0.643      | 0       |
| Collimator size (cm) |         | Source to Target Distance (cm) |        | 6 MVe      |            |         |
|                      |         |                                |        | $\alpha_1$ | $\alpha_2$ | $\beta$ |
| 1.0                  |         | 90                             |        | 0.224      | 0.562      | 0.110   |
|                      |         | 100                            |        | 0.342      | 0.680      | 0.119   |
|                      |         | 120                            |        | 0.464      | 0.100      | 0.248   |
| 1.2                  |         | 83                             |        | 0.214      | 0.372      | 0.0129  |
|                      |         | 100                            |        | 0.392      | 0.613      | 0.0533  |
|                      |         | 114                            |        | 0.225      | 0.953      | 0.197   |
| 1.4                  |         | 85                             |        | 0.370      | 0.448      | 0.0024  |
|                      |         | 100                            |        | 0.546      | 0.696      | 0.0244  |
|                      |         | 114                            |        | 0.552      | 0.934      | 0.0862  |
| Collimator size (cm) |         | Source to Target Distance (cm) |        | 8 MVe      |            |         |
|                      |         |                                |        | $\alpha_1$ | $\alpha_2$ | $\beta$ |
| 1.0                  |         | 90                             |        | 0.358      | 0.558      | 0       |
|                      |         | 100                            |        | 0.303      | 0.959      | 0       |
|                      |         | 120                            |        | 0.574      | 1.030      | 0       |
| 2.0                  |         | 90                             |        | 0.413      | 0.453      | 0       |
|                      |         | 100                            |        | 0.517      | 0.608      | 0       |
|                      |         | 120                            |        | 0.689      | 0.792      | 0       |
| 3.0                  |         | 90                             |        | 0.347      | 0.361      | 0       |
|                      |         | 100                            |        | 0.490      | 0.550      | 0       |
|                      |         | 120                            |        | 0.651      | 0.806      | 0       |
| 4.0                  |         | 90                             |        | 0.377      | 0.363      | 0       |
|                      |         | 100                            |        | 0.470      | 0.502      | 0       |
|                      |         | 120                            |        | 0.672      | 0.681      | 0       |
| Energy               | $Q_1$   | $Q_2$                          | $Q_3$  | $Q_4$      | $Q_5$      | $Q_6$   |
| 6 MeV                | -0.577  | 0.0117                         | -1.005 | 0.0165     |            |         |
|                      | -0.0447 | 0.00359                        | -1.005 | 0.0165     | -0.433     | 0.00547 |
| 8 MeV                | -0.478  | 0.0099                         | -0.651 | 0.0125     |            |         |

value of 0.02 was used for  $t$ . Most of the fitting curves agree well with measured data except for smaller collimators.

The addition of a quadratic term to the exponent for the inner penumbra description gives an

improvement to field sizes smaller than 1.4 cm. This makes it possible to create profiles which have a flat maximum in the center, while maintaining the appropriate gradient in the penumbra region for the small collimator.

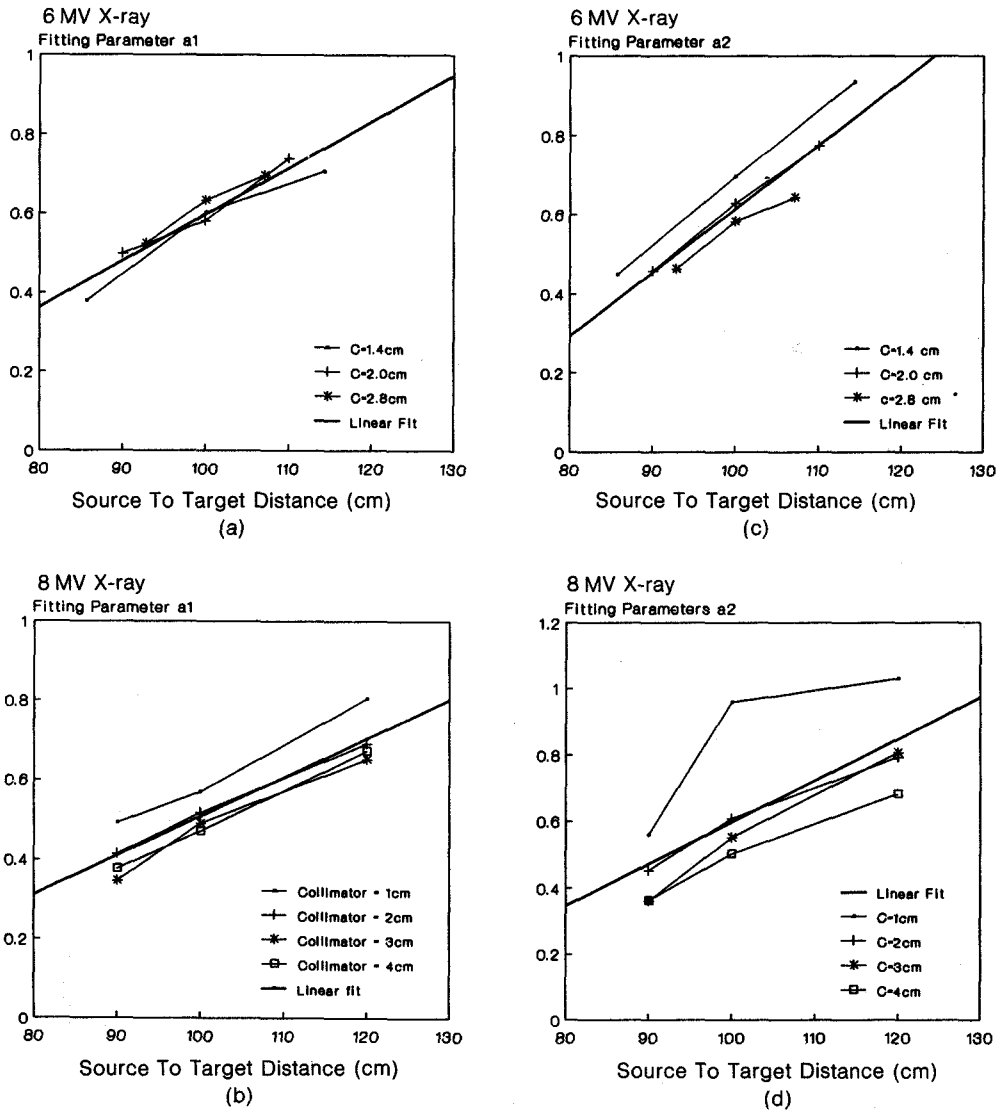


Fig. 9. Fitting parameters  $\alpha_1$  and  $\alpha_2$  with composite linear regression. The thin solid lines represent the trends of individual fitting parameters,  $\alpha_1$  and  $\alpha_2$  for different collimator sizes and STDs. The thick solid lines denote the composite linear regression for multi-collimators.

Fig. 9 shows trends of the fitting parameters  $\alpha_1$  and  $\alpha_2$  with the variation of STD and collimator size for two different beam energies. There are several options to determine fitting parameters for any collimator size and STD. One direct method is to interpolate between known parameters. Another is to find the relationship between fitting parameters and beam parameters such as collimator size or STD. Figure 9 also shows composite linear regression of  $\alpha_1$  and  $\alpha_2$  with STD for multi-collimators

ignoring the collimator dependence of  $\alpha_1$  and  $\alpha_2$ . Figure 10 shows another composite linear regression for multi-collimators for 6 MVX with film measurement. The formula for OAR now can be generalized with new expressions for  $\alpha_1$  and  $\alpha_2$ :

$$\alpha_1 = Q_1 + Q_2 \text{ STD} \dots\dots\dots(9)$$

$$\alpha_2 = Q_3 + Q_4 \text{ STD} \dots\dots\dots(10)$$

with an additional expression for small collimators ( $C < 1.4$  cm):



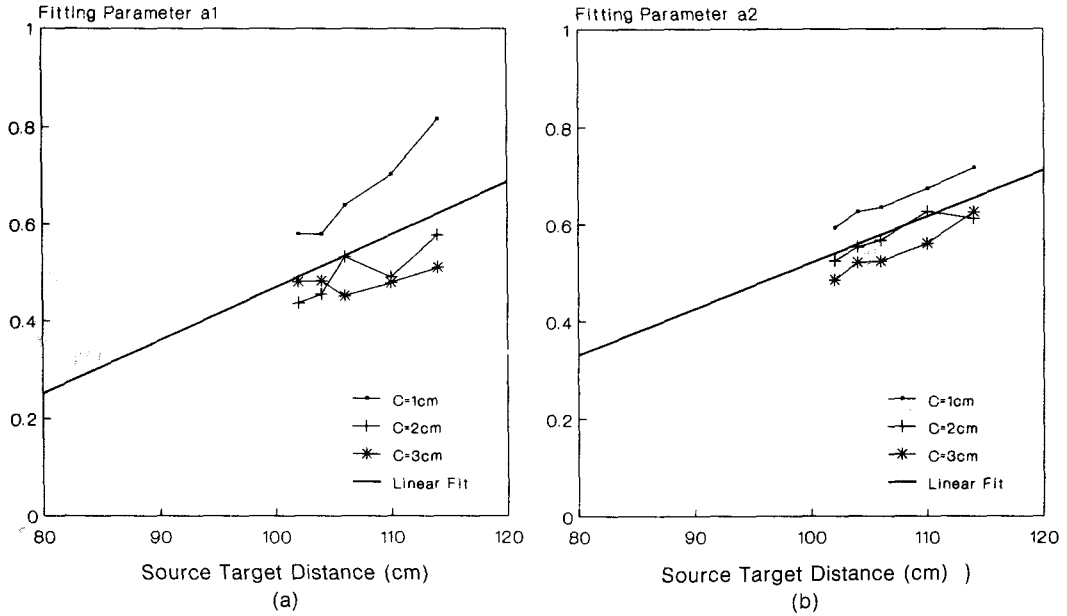


Fig. 10. Fitting parameters  $\alpha_1$  and  $\alpha_2$  vs. source-to-target distance for collimator size of 1, 2, 3 cm with measurement. (a)  $\alpha_1$  for 6 MeV X-ray, (b)  $\alpha_2$  for 6 MeV X-ray.

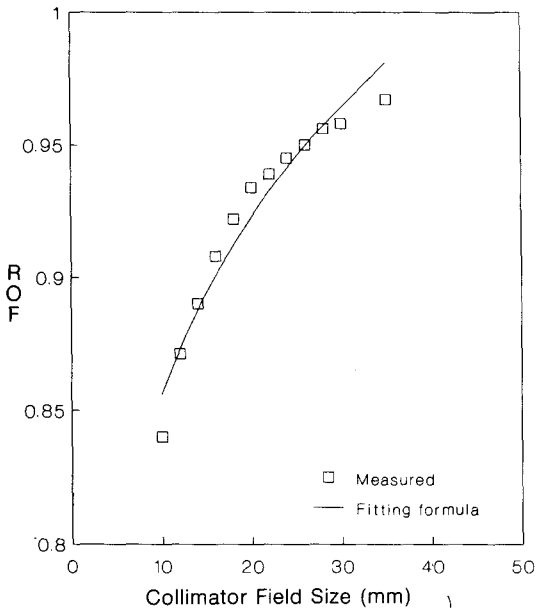


Fig. 11. Relative output factors vs. collimator settings. Collimator settings define the field size at isocenter. The points denote measured data, the curves denote least square fit.

$\beta = Q_s + Q_s \text{ STD} \dots\dots\dots(11)$   
 The coefficients of regression are shown in table

2. A formula may be derived from the biquadratic form which includes dependence on both collimator size and STD. However, this is not recommended as more parameters only provide a minimal increase in the accuracy of the expression.

**3. Relative Output Factor**

To express the relationship between dose and monitor units for different collimator sizes, relative output factors (ROF) are used. The relative output factor was measured at  $d_{\max}$  with source-to-chamber distance of 100 cm with the Reference setup (source-to-surface distance of 100 cm at  $d_{\max}$  for field size of  $10 \times 10$  cm). Figure 11 shows the measured ROF for different collimator sizes. The ROF data may be fit to a function of the form:

$\text{ROF} = S_1 \times C^{S^2} \dots\dots\dots(12)$

The final dose model for a single circular field is:

$D(C, \text{STD}, d, r) = D_{\text{Ref}} \times \text{ROF}(C) \times \text{TMR}(w, d) \times (\text{SAD}/\text{STD})^2 \times \text{OAR}(C, \text{STD}, r) \dots\dots\dots(13)$

where all function values are explicitly represented by the formulae developed here.

**CONCLUSION**

The result of this study indicate that our simple beam data collection techniques for small beams

provide adequate data that can be used for stereotactic radiosurgery planning for any energy of photon beams. The measured TMRs and OARs for 6 and 8 MV X-ray beams could be represented by a simple approximate analytic form which is convenient and very efficient to use for generating basic beam data for any possible set-up conditions. The advantage of this analysis system for small beam measurement can reduce not only measuring time but also human or device error during measurement. However, detector size and positioning were most important factors in making precise measurements and obtaining good trends of measured beam data.

### REFERENCES

1. Colombo F, Benedetti A, Pozza F, et al: External Stereotactic Irradiation by Linear Accelerator, Neurosurgery, 16:154, 1985
2. Hartmann GH, Schlegel W, Sturm V, et al: Cerebral Radiation Surgery Using Moving Field Irradiation at a Linear Accelerator Facility. Int J Radiat Oncol Biol Phys 11:1185, 1985
3. Heiftz MD, Wexler M, Thompson R: Single Beam Radiotherapy Knife; A practical Theoretical Model. J Neurosurg 60:814, 1984
4. Lutz W, Winston KR, Maleki N: A System for Stereotactic Radiosurgery with a Linear Accelerator. Int J Radiat Oncol Biol Phys 14:373, 1988
5. Pike B, Podgorsak EB, Peters TM, et al: Dose distributions in dynamic stereotactic radiosurgery. Med Phys 14:780, 1987
6. Friedman WA, Bova FJ: The University of Florida Radiosurgery System. Surg Neurol 32:334, 1989
7. Houdck PV, Vanburen J, Fayos JV: Dosimetry of Small Radiation Fields for 10 MV X rays. Med Phys 4:333, 1983
8. Rice RK, Hansen JL, Svensson GK, et al: Measurement of Dose Distribution in Small Beams of 6 MV X-ray. phys Med Biol 32:1087, 1987
9. Khan FM, Sewchand W, Lee J, et al: Revision of Tissue-Maximum Ratio and Scatter-Maximum Ratio Concepts for Cobalt 60 and Higher Energy X-Ray Beams. Med Phys 7:230, 1980
10. Dixon RL, Ekstrand KE, Huff WJ: Beam Characteristics of the Varian 6 MV Clinac 6X Accelerator. Int J Radiat Oncol Biol Phys 2:585, 1977
11. Van Dyk J: Practical dosimetric considerations of a 10 MV photon beam. Med Phys 4:145, 1977
12. Johns HE, Cunningham JR: The Physics of Radiology, Charles C. Thomas Springfield IL, pp 416-419, (1983)

== 국문초록 ==

### Philips LINAC 6 MV와 8 MV X선 소조사면에 대한 선량분포 측정

가톨릭 의과대학 방사선과학교실

서태석 · 윤세철 · 신경섭 · 박용휘

본 논문에서는 소조사면에 대한 X-선의 선량분포를 일반실험식으로 계산될 수 있도록 beam 측정 데이터를 종합 처리하는 방법에 대하여 기술하고 있다. Beam 데이터는 philips LINAC 6 MV, 8 MV X-ray에 대하여 측정 되었으며, 측정된 요소는 tissue maximum ratio (TMR), off-axis-ratio (OAR), 그리고 relative output factor (ROF)를 포함한다.

소조사면에 의한 방사선 치료를 위하여 isocenter에서 지름이 1 내지 3 cm 되도록 실린더 형태의 특수 collimator가 2 mm 간격으로 제작되었다. 본 측정을 위하여 다이오드 detector가 이용되었으며 Film 및 TLD 측정기로 측정된 값과 비교검토 되었다.

제한된 조사면으로 측정된 TMR, OAR data로부터 beam 데이터를 나타내는 실험식을 유도하였으며 이 실험식은 임의의 set-up조건에 따른 측정값을 예상할 수 있는 일반 실험식으로 확장되었고 측정된 TMR과 OAR 값들은 잘 일치되었다.